Generation, Characterization and Manipulation of Quantum Correlations in Electron Beams

-- SUPPLEMENTARY INFORMATION --

Shahaf Asban[1,*] and Javier García de Abajo[1,2,†]

[1] *ICFO - Institut de Ciencies Fotoniques, The Barcelona Institute of Science and Technology, 08860 Castelldefels (Barcelona), Spain*
[2] *ICREA - Institució Catalana de Recerca i Estudis Avançats, Passeig Lluís Companys 23, 08010 Barcelona, Spain*

In this document we formulate the framework and derive the pair amplitude explored in the main text. We provide a brief overview of macroscopic electrodynamics, then employ it to introduce the polariton field. Using the minimal coupling field-electron coupling we obtain the pair amplitude pertubatively. Schmidt decomposition and the coincidence probability of the pair are also reviewed.

We consider two beam electrons moving in proximity of a medium of permittivity $\epsilon(\boldsymbol{r},\omega)$. We use the macroscopic QED formalism, closely following the scheme presented in Ref. [1], using the current operator as a bosonic joint light-matter operator characterized by the losses of the electromagnetic field:

$$\hat{\mathbf{j}}(\mathbf{r},\omega) = \frac{\omega}{4\pi c}\sqrt{4\hbar\Im\mathfrak{m}\{\epsilon\}(\mathbf{r},\omega)}\hat{\mathbf{f}}(\mathbf{r},\omega), \tag{1}$$

$$\left[\hat{\mathbf{f}}(\mathbf{r},\omega),\hat{\mathbf{f}}(\mathbf{r}',\omega')\right] = \left[\hat{\mathbf{f}}^\dagger(\mathbf{r},\omega),\hat{\mathbf{f}}^\dagger(\mathbf{r}',\omega')\right] = 0, \tag{2}$$

$$\left[\hat{f}_i(\mathbf{r},\omega),\hat{f}_j^\dagger(\mathbf{r}',\omega')\right] = \delta_{ij}\delta(\omega-\omega')\delta(\mathbf{r}-\mathbf{r}'). \tag{3}$$

The Hamiltonian then assumes the diagonal form in this basis,

$$\hat{H}_\phi = \int d^3\mathbf{r}\int_0^\infty d\omega'\,\hbar\omega\hat{\mathbf{f}}^\dagger(\mathbf{r},\omega)\cdot\hat{\mathbf{f}}(\mathbf{r},\omega). \tag{4}$$

The field operator in the Schrodinger picture is given by,

$$\hat{\mathbf{A}}(\mathbf{r}) = 4\pi c\int_0^\infty d\omega\int d^3\mathbf{r}'\mathcal{G}(\mathbf{r},\mathbf{r}',\omega)\hat{\mathbf{j}}(\mathbf{r}',\omega) + H.c., \tag{5}$$

where the Green tensor is given by the solution of,

$$\nabla\times\nabla\times\boldsymbol{\mathcal{G}}(\mathbf{r},\mathbf{r}',\omega) - \frac{\omega^2}{c^2}\epsilon(\mathbf{r},\omega)\boldsymbol{\mathcal{G}}(\mathbf{r},\mathbf{r}',\omega) = 4\pi\mathbb{1}^{(3)}\frac{\omega^2}{c^2}\delta(\mathbf{r}-\mathbf{r}').$$

The full Hamiltonian is given by,

$$H = H_\phi + H_\mathrm{e} + H_\mathrm{I} = H_0 + H_\mathrm{I}, \tag{6}$$

where,

$$H_\mathrm{e} = \sum_{\mathbf{k},s}\epsilon_{\mathbf{k}}c_{\mathbf{k},s}^\dagger c_{\mathbf{k},s}, \tag{7}$$

$$H_{\mathrm{e}-\phi} = \frac{e\lambda_\mathrm{C}}{2\pi}\sum_{\mathbf{k},\mathbf{q},\sigma}c_{\mathbf{k}+\mathbf{q},s}^\dagger c_{\mathbf{k},s}\mathbf{k}\cdot\hat{\mathbf{A}}(\mathbf{q}), \tag{8}$$

* Shahaf.S.Asban@gmail.com

† Javier.GarciaDeAbajo@nanophotonics.es

$\lambda_{\mathrm{C}} = {}^{h}/_{m_{\mathrm{e}}c}$ is the electron Compton wavelength and m_{e} and e are the mass and charge. Also, we define the Fourier transform of the vector-field using,

$$\hat{\mathbf{A}}\left(\mathbf{q}\right) = L^{-3}\int d^{3}\mathbf{r}e^{-i\mathbf{q}\cdot\mathbf{r}}\hat{\mathbf{A}}\left(\mathbf{r}\right).$$

We adopt the Weyl gauge, in which the scalar field is set as zero.

The pair amplitude.– We assume an initial product state, reflecting complete separability:

$$\left|\Psi_{0}\right\rangle = \int_{\Omega} dk_{1}dk_{2}\,\alpha_{s_{1}}^{(1)}\left(\boldsymbol{k}_{1}\right)\alpha_{s_{2}}^{(2)}\left(\boldsymbol{k}_{2}\right)c_{\boldsymbol{k}_{1},s_{1}}^{\dagger}c_{\boldsymbol{k}_{2},s_{2}}^{\dagger}|0_{1},0_{2}\rangle_{\mathrm{e}}|\otimes|\alpha\rangle_{\mathrm{p}}, \tag{9}$$

where $\alpha_{s_{i}}\left(\boldsymbol{k}_{i}\right)$ is a single electron distribution of momentum and spin $\boldsymbol{k}_{i}, s_{i}$, and the polaritons are prepared in the initial state $|\alpha\rangle$. We are interested in the interacting (two-electron) subspace given by

$$\langle\alpha|\Psi^{(2)}\left(T\right)\rangle = -\frac{1}{2\hbar^{2}}\mathcal{T}\left\{\int dt_{2}dt_{1}\mathcal{H}_{\mathrm{e}-\phi}\left(t_{2}\right)\mathcal{H}_{\mathrm{e}-\phi}\left(t_{1}\right)\right\}|\Psi_{0}\rangle, \tag{10}$$

where $\mathcal{T}$ is the time-ordering superoperator and $\mathcal{H}_{\mathrm{e}-\phi}\left(t_{i}\right)$ is the interaction Hamiltonian. The above operators evolved using the noninteracting field Hamiltonians. Note that $\mathbf{A}\left(\boldsymbol{r}\right)$ contains two terms obeying the commutation relations 3. Adding together Hermitian conjugates as a result of time ordering yields $\delta_{ij}\delta\left(\omega_{1}-\omega_{2}\right)\delta\left(\mathbf{r}_{1}-\mathbf{r}_{2}\right)$. We further use the relation [1],

$$\frac{\omega^{2}}{c^{2}}\int d^{3}\mathbf{s}\epsilon_{\mathrm{I}}\left(\mathbf{s},\omega\right)\mathcal{G}_{ki}\left(\mathbf{s},\mathbf{r},\omega\right)\mathcal{G}_{kj}^{*}\left(\mathbf{s},\mathbf{r}',\omega\right) = \frac{1}{2i}\left[\mathcal{G}_{ij}\left(\mathbf{r},\mathbf{r}',\omega\right)-\mathcal{G}_{ij}^{*}\left(\mathbf{r},\mathbf{r}',\omega\right)\right], \tag{11}$$

then trace the lateral dimensions (x, y) of Eq. 10, and from here obtain the general form given in Eq. (1) of the main text:

$$|\Psi^{(2)}\left(T\right)\rangle_{\lambda} = \sum_{\boldsymbol{k}_{1}\boldsymbol{k}_{2}}\Phi_{s_{1}s_{2}}^{\lambda}\left(k_{1},k_{2};T\right)|k_{1},s_{1};k_{2},s_{2}\rangle, \tag{12}$$

where we have defined Eq. (1) of the main text

$$\Phi_{s_{1}s_{2}}^{\lambda}\left(k_{1},k_{2};T\right) = \mathcal{N}^{-1/2}\int dq\,\mathrm{sinc}\left[\frac{\hbar q}{m}\left(k_{1}-k_{2}\right)T\right]\chi\left(q\right)\alpha_{s_{1}}^{(1)}\left(\boldsymbol{k}_{1}-q\right)\alpha_{s_{2}}^{(2)}\left(\boldsymbol{k}_{2}+q\right). \tag{13}$$

In the integration we have invoked the nonrecoil approximation introduced in the main text for the dispersion difference, $\omega_{\boldsymbol{q}_{\mathrm{i}}} = \omega_{\boldsymbol{k}_{\mathrm{i}}+\boldsymbol{q}_{\mathrm{i}}}-\omega_{\boldsymbol{k}_{\mathrm{i}}}$. Also, we have made use of the notation $\boldsymbol{r} = \boldsymbol{r}_{1}-\boldsymbol{r}_{2}/2$ and $\boldsymbol{R} = \boldsymbol{r}_{1}+\boldsymbol{r}_{2}/2$, where $\boldsymbol{r}$ is the conjugate coordinate used in the Fourier transform of the Green tensor. The factor $\chi\left(q\right)\equiv\chi\left(q_{z}\right)$ is the Fourier transform of the Green tensor, traced with respect to the y, z components. The evanescent nature of the field introduce exponential decay with respect to the distance from the medium y_{0} [1, 2]). Taking the long l_{x} limit (see Fig. 1) conveniently reduces the integration dimension by generating a delta-function distribution $\delta\left(q_{x_{1}}+q_{x_{2}}\right)$. We are interested in the dynamics along the propagation direction, which is formally given by entirely tracing out the lateral dimensions. We consider Gaussian initial states of mean distance $y_{0} = 5\,\mathrm{nm}$ from the thin film and $\sigma_{y} = 0.5\,\mathrm{nm}$ (see Fig. 1 in the main text). The behavior of $\chi\left(q\right)$ is dominated by the Gaussian, inherited from the x, y components of the wave-function. The coupling resonates when the polariton dispersion intersects the electron line $\omega = \boldsymbol{q}\cdot\boldsymbol{v}$. We have chosen $\sigma_{x} = \frac{2\pi}{\lambda_{\mathrm{p}}}$, where λ_{p} is the natural lengthscale providing the dominant polariton wavelength. It is taken to be the point in which the polariton dispersion intersects the electron dispersion, and thus vary with the electron velocity as Depicted in Fig. 1. Clearly, the initial momenta distribution along the x, y directions affects the dominant integration domain and can be used as an additional control parameter that is outside the scope of this work.

Schmidt decomposition and temporal modes.– The Schmidt decomposition allows one to express an inseparable state as a coherent superposition of separable eigenstates. We denote the eigenstates of the reduced density matrix as *temporal modes* when the amplitude can be described by the longitudinal momentum component. In other words, when the electron is well collimated along the transverse dimensions relative to its propagation direction. Along with the none recoil approximation, in which we consider fixed velocity, the energy exchange results in a leading linear

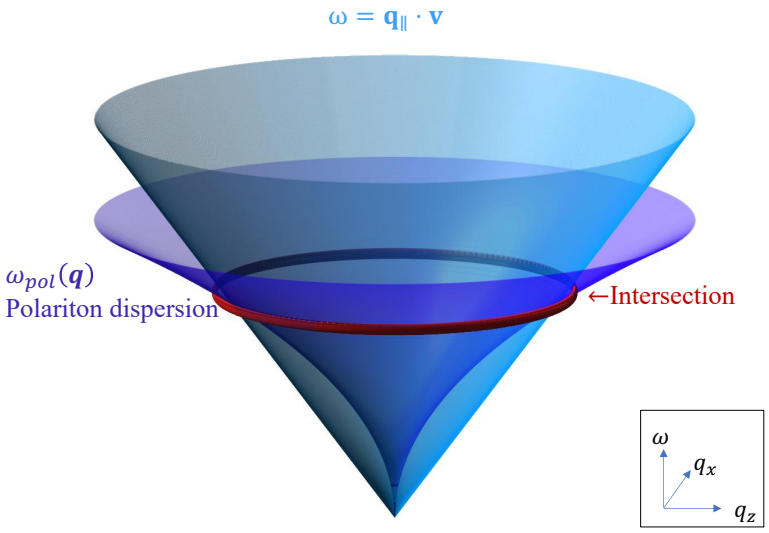

Figure 1. The polariton dispersion $\omega_{\mathrm{pol}}(\boldsymbol{q})$ and its intersection with the electronic conical surface $\boldsymbol{q}\cdot\boldsymbol{v}$. The red area indicates $\lambda_p = {}^{2\pi}/_{q_p}$ where maximal coupling occurs, providing a natural lengthscale in our analysis .

contribution to the momentum exchange. Thus, the momentum-position relations are interpreted as a time-energy interplay, similar to the photonic counterpart studied in [3, 4]. To obtain the temporal Schmidt mode decomposition, we use the Schmidt-Mercer theorem, so the inseparable pair amplitude can be expressed as,

$$\Phi^{\lambda}_{s_1 s_2}(k_1, k_2) = \sum_n \sqrt{p_n}\psi_n(k_1)\,\phi_n(k_2)\,, \tag{14}$$

where we have omitted the spin labels for brevity. The eigenfunctions are obtained from the integral equations,

$$\psi_n(k) = \frac{1}{p_n}\int dk'\, K_1(k,k')\,\psi_n(k')\,, \tag{15}$$

$$\phi_{n,}(k) = \frac{1}{p_n}\int dk'\, K_2(k,k')\,\phi_n(k')\,, \tag{16}$$

and the kernels are given by,

$$K_1(k,k') = \int dk_2\,\Phi(k,k_2)\,\Phi^*(k',k_2)\,, \tag{17}$$

$$K_2(k,k') = \int dk_1\,\Phi(k_1,k)\,\Phi^*(k_1,k')\,. \tag{18}$$

These quantities bear all the required single-particle information and may be interpreted as a single-particle correlation functions, while ϕ_n and ψ_n are single particle amplitudes. In this sense, the corresponding weights λ_n express the probability of measuring one electrons in the n^{th} Schmidt mode. In this study, we find that $\psi_n = \phi_n^*$ due to the symmetry in the interaction term combined with the respective parameters chosen for the two electrons. This differs from the scenario presented by photonic time-frequency entanglement, where the left and right eigenfunction are distinct ($\psi_n \neq \phi_n^*$). In the photonic case this stems from the fact that different polarizations travel with different velocities in a nonlinear crystal. These modes hold two important (and computationally useful) properties: orthogonality and completeness which can be expressed as

$$\delta_{nm} = \int dk\,\psi_n(k)\,\phi_m(k)\,, \tag{19}$$

$$\delta(k_1 - k_2) = \sum_n \psi_n(k_1)\,\phi_n(k_2)\,. \tag{20}$$

Coincidence Probability.– The Schmidt modes are essentially eigenstates of the reduced one-electron density matrix. In each realization of the experiment, the electrons are found to be in a similar Schmidt mode $\phi_n(k)$ with probability $\sqrt{p_n}$, resulting in the wave-function

$$|\Psi\rangle = \sum_n \sqrt{p_n}\phi^*_{n,\sigma_1}(\boldsymbol{k}_1)\,\phi_{n,\sigma_2}(\boldsymbol{k}_2)\,|\boldsymbol{k}_1\sigma_1;\boldsymbol{k}_2\sigma_2\rangle. \tag{21}$$

We consider the configuration described Fig. 3a of the main text, corresponding to an electronic Hong-Ou-Mandel interference of electrons. The fermion-field beam-splitter transformation can be represented by (in frequency domain)

$$\begin{pmatrix} \Psi_{a'} \\ \Psi_{b'} \end{pmatrix} = \begin{pmatrix} \sqrt{\mathcal{T}} & i\sqrt{\mathcal{R}}e^{i\omega\Delta} \\ i\sqrt{\mathcal{R}}e^{-i\omega\Delta} & \sqrt{\mathcal{T}} \end{pmatrix} \begin{pmatrix} \Psi_a \\ \Psi_b \end{pmatrix}, \tag{22}$$

where $\Delta = {}^{\delta l}/_{v}$ is the relative time difference in generated by a shift in the BS position δl and v the electron velocity. The coincidence probability is then calculated from the expression

$$\mathcal{P}_{12}(\Delta) = \int dt\, d\tau \left\langle \Psi^\dagger_{a''}(t)\,\Psi^\dagger_{b''}(t+\tau)\,\Psi_{b''}(t+\tau)\,\Psi_{a''}(t)\right\rangle, \tag{23}$$

where the double prime notation corresponds to two BSs arrangement specified as indicated in Fig. 2a. Plugging in the wave-function in the Schmidt basis, we obtain

$$\mathcal{P}_{12}(\Delta) = \mathcal{R}^2 + \mathcal{T}^2 + 2\mathcal{R}\mathcal{T}\sum_{np}\sqrt{p_n p_p}\,|\mathcal{I}_{np}(\Delta)|^2,$$

where we have defined the freely propagating Schmidt modes overlap,

$$\mathcal{I}_{np}(\Delta) = \int dk\,\phi^*_n(k)\,\phi_p(k)\,e^{-\frac{i}{\hbar}E_k\Delta}, \tag{24}$$

with respect to the free fermion kinetic energy E_k. Note that the momentum summation includes only one component along the propagation direction, compatible with the nonrecoil linearization scheme indicated above. For balanced BS we obtain the expression presented in Fig. 2a-b of the main text,

$$\mathcal{P}_{12}(\Delta) = \frac{1}{2} + \frac{1}{2}\sum_{np}\sqrt{p_n p_p}\,|\mathcal{I}_{np}(\Delta)|^2. \tag{25}$$

Interestingly, in the special case in which $\Delta = 0$, we find that $\mathcal{I}_{np}(0) = \delta_{np}$ and the interference pattern reduces to $\sum_n p_n = 1$. This recovers the well-known result of identical fermion Hong-Ou-Mandel interference leading to complete unity coincidence probability. We use this property next for state characterization - coincidence-based temporal mode discrimination and tomography.

Fig. 3b of the main text reveal the coincidence probability as a function of the Schmidt number κ. The inset of the left panel clearly exhibits two regimes of linear dependence of κ and T_I. This points towards a crossover between two different rates of mode-production. The Schmidt number provides an indication for the effective Hilbert-space dimension. The pair amplitude is obtained by integrating the input wave-packets with $\chi(q)$, which is the convolution between the y component of the electrons wave function and the polariton resonance peak. The transition is visible when the variance (width) of $\chi(q) \to \delta\chi_q^2$ is proportional to the initial wave-packet width, $\delta\chi_q^2 \approx \sigma_e^2$. This regime is inaccessible pertubatively, unlike $\sigma_{\rm e}^2 \gg \delta\chi_q^2$ or $\sigma_{\rm e}^2 \ll \delta\chi_q^2$ (for which no transition occurs), and thus challenging to be treated analytically. Interestingly, the Von Neumann entropy $S_{VN} = -\sum_k p_k \log_2 p_k$ is smooth throughout this crossover.

Temporal mode identification and state tomography.– We consider the configuration described Fig. 3a of the main text, corresponding to an electronic Hong-Ou-Mandel interferometer in a similar fashion as described in the section above.In contrast to the previous section, the incoming instantaneous interference includes one electron from the entangled pair ϕ_n and a probe prepared in the state ϕ_p, as depicted in Fig. 4 of the main text. The coincidence of a prepared (probe) electronic state ϕ_p with the incoming single electron in state ϕ_n is given by,

$$\mathcal{P}_{12}(\Delta) = \frac{1}{2} + \frac{1}{2}\left|\mathcal{I}_{np}(\Delta)\right|^2. \tag{26}$$

Figure 4 in the main text is calculated from this expression. Since the temporal electronic modes are eigenvalues of the reduced density matrix, in each detection event of the experiment, we expect to realize one of these states with a corresponding probability p_n. When $n = p$, we obtain information regarding the incoming mode via this jump in the observable. This information describes the collapse of the entangled counterpart fermion field (in the other port) to the same known state. Repeating this protocol multiple times, the arrival rate convergence of each mode will reveal the mode probability, which characterizes the entanglement.

---

[1] Ho Trung Dung, Ludwig Knöll, and Dirk-Gunnar Welsch. Three-dimensional quantization of the electromagnetic field in dispersive and absorbing inhomogeneous dielectrics. *Phys. Rev. A*, 57:3931–3942, May 1998.

[2] Stefan Yoshi Buhmann. *Dispersion Forces I.* Springer-Verlag Berlin Heidelberg, 2012.

[3] Michael G Raymer and Ian A Walmsley. Temporal modes in quantum optics: then and now. *Physica Scripta*, 95(6):064002, mar 2020.

[4] B. Brecht, Dileep V. Reddy, C. Silberhorn, and M. G. Raymer. Photon temporal modes: A complete framework for quantum information science. *Phys. Rev. X*, 5:041017, Oct 2015.